Membrane Flux through the Pore Formed by a Fusogenic Viral Envelope Protein during Cell Fusion

F. W. Tse, A. Iwata, and W. Almers*

Dept. of Physiology and Biophysics, University of Washington, Seattle, Washington 98195; and *Max-Planck Institut für Medizinische Forschung, Abt. Molekulare Zellforschung, 6900 Heidelberg, Germany

Abstract. We have investigated the mechanism of cell fusion mediated by HA, the fusogenic hemagglutinin of the *Influenza* viral envelope. Single erythrocytes (RBCs) were attached to fibroblasts expressing the HA on their cell surface, and fusion of the paired cells was triggered by rapid acidification. The RBC membrane was stained with fluorescent lipid, and the fusion-induced escape of lipid into the fibroblast was observed by quantitative image analysis. At the same time, the formation of an aqueous connection (i.e., the fusion pore) between the two cells was monitored electrically. Within minutes after acidification, an electrical conductance between the two cells appeared abruptly as the fusion pore opened, and then increased gradually as the pore dilated. Later, fluorescent lipid diffused into the fibroblast, approaching equilibrium over the next 5–20 min. No lipid flux was seen while the pore conductance remained 0.5 nS or less. Evidently lipid flux requires a threshold pore size. Our finding suggests that the smallest and earliest fusion pores are surrounded by a ring of protein. A fusion pore expands by breaking this ring and recruiting lipid into its circumference.

MEMBRANE fusion is a fundamental event in cell biology, and is probably mediated by a variety of fusogenic (or fusion) proteins. Among fusion proteins, the hemagglutinin (HA)[1] of the *Influenza* virus is the best characterized, both on a structural (Wiley and Skehel, 1987) and functional level (Stegmann et al., 1989; White, 1990; Stegmann et al., 1991). Once HA has been made fusion competent by proteolytic cleavage, acidification triggers a structural change that makes HA transiently fusogenic. Although the structure of HA at neutral pH is known at atomic resolution (Wiley and Skehel, 1987), the structure generated by acidification is not. The mechanisms of biological fusion in general, and of HA-mediated fusion in particular, remain unclear.

Single fusion events may be observed when fibroblasts transfected with HA are allowed to fuse to attached RBCs (Doxsey et al., 1985). These studies have shown that an early event in HA-induced fusion is the formation of a "fusion pore" (Sarkar et al., 1989; Spruce et al., 1989, 1991), an aqueous connection between the fusing cells whose electrical conductance (and, hence, diameter) is initially no larger than that of a large ion channel (Spruce et al., 1989, 1991). The fusion pore later expands, presumably by incorporation of lipid. Similar findings have been made during exocytosis in mast cells. While early states of the fusion pore may be similar to an ion channel (Breckenridge and Almers, 1987; Spruce et al., 1990), later states allow the flux of lipid membrane from one compartment to the other (Monck et al., 1990). Lipid flux along the fusion pore may thus be used as a diagnostic for the composition of the pore.

To see whether and when HA-mediated fusion pores begin to pass lipid, we have compared the time course of lipid mixing and the development of cytoplasmic continuity. One such study (Sarkar et al., 1989) monitored the dequenching of two fluorescent probes, one water and the other lipid soluble, in suspensions of fusing cells loaded with both probes. Lipid mixing and cytoplasmic continuity appeared to occur simultaneously. However, in cell suspensions, the multitude of fusion events cannot be expected to occur in synchrony, and differences in the timing of lipid mixing and cytoplasmic continuity during individual fusion events could be obscured. Here we have used a combination of patch clamp and video imaging to monitor the fusion of single cell pairs. Cytoplasmic continuity developed minutes before lipid mixing began. Preliminary accounts of this work have been included elsewhere (Almers et al., 1991).

Materials and Methods

Cell Culture and Cell Activation

Fresh human RBCs were washed, diluted (hematocrit 1%), and stained with fluorescent lipid, either *N*-(Texas red sulfonyl)-dipalmitoyl-L-α-phosphatidylethanolamine (TR-DPPE) or 1,1′-dioctadecyl-3,3,3′,3′-tetramethylindodicarbocyanine (di-I). Fluorescent lipids were from Molecular Probes

1. *Abbreviations used in this paper*: C, capacitance; HA, hemagglutinin; RBC, human erythrocyte; di-I, 1,1′-dioctadecyl-3,3,3′,3′-tetramethylindodicarbocyanine; TR-DPPE, *N*-(Texas Red sulfonyl)-dipalmitoyl-L-α-phosphatidylethanolamine.

Inc. (Eugene, OR) and kept as an ethanolic stock (1 mg/ml) at −80°C. RBC suspensions were incubated for 30 min at 25°C in PBS with 1–2 μl/ml of lipid stock solution added. Under whole cell voltage clamp, RBCs so stained had a membrane capacitance of 930 ± 36 fF (± SEM, n = 5; 2RBCs stained with TR-DPPE, 3 with di-I), similar to the value obtained with unstained RBCs (910 ± 20 fF; Spruce et al., 1989). RBCs were either used immediately, or within <48 h at 4°C. RBCs stored longer were too leaky for electrical recording.

Fibroblasts stably expressing HA in their plasma membrane (NIH-3T3HA-b2; Ellens et al., 1990) were grown at 5% CO_2 (37°C) to 30–60% confluency on glass coverslips in growth medium (DME; GIBCO BRL, Gaithersburg, MD) supplemented with 10% FBS, 100 U/ml penicillin and 100 μg/ml streptomycin (all from GIBCO BRL). To cleave the HA to its fusion-competent form, cells were washed in PBS, incubated for 4 min (25°C) in trypsin-containing serum-free growth medium (10 μg/ml), and then washed in growth medium and returned to the incubator. After 15–120 min individual coverslips were removed and the fibroblasts were allowed to bind RBCs as described (Spruce et al., 1989). The coverslip was then placed in the experimental chamber containing a Ca-free saline (in mM, 155 *N*-methyl-glucamine glutamate, 5 $MgCl_2$, 2 Cs-Hepes, pH 7.4) with the usual NaCl and KCl replaced by large and presumably impermeant organic ions. This was done to suppress a reversible conductance increase in the fibroblast membrane that accompanies acidification in NaCl buffer (Spruce et al., 1989). Fusion was triggered by pressure ejection of acidic buffer from a glass micropipette (tip diameter 3 μm) placed within 100 μm of the RBC–fibroblast cell pair. In this solution, 20 mM succinate (pH 4.8) replaced the 2 mM Cs-Hepes buffer in the external solution. Experiments on RBCs stained with TR-DPPE were done at 30 ± 1°C; experiments with di-I at 27 ± 1°C.

To test the fusion competence of HA-expressing fibroblasts, we subjected them to proteolysis as described above, triggered fusion by external acidification (pH 4.8 for 3 min at 37°C), returned them to the incubator for 15 min (37°C), and then examined for fluorescence all fibroblasts that had bound one RBC. With all batches of RBCs and fibroblasts, more than 86% of the fibroblasts became fluorescent, indicating lipid mixing between the bilayers of the cell pair. If either trypsin treatment or acidification was omitted, transfer of TR-DPPE or di-I to the fibroblast was never observed (n = 200).

Electrical Recording

Whole-cell recordings were made from fibroblasts with glass micropipettes coated with silicone resin (Hamill et al., 1981) and filled with a solution containing, in mM, 155 Cs-glutamate, 5 $MgCl_2$, 5 BAPTA, 10 Cs-Hepes, pH 7.4. Pipettes had 1.5–4-MΩ resistances and made 3–11-MΩ connections with the cytosol. We selected small (8.3–24 pF of plasma membrane capacitance), solitary fibroblasts that had bound a single RBC at their margin. The fibroblasts were voltage clamped at a DC holding potential of 0 mV. The capacitance of the plasma membrane was measured by applying square voltage pulses and carefully nulled out. Voltage steps (10 mV, 0.5 s) were then applied repeatedly at 1 Hz, and the DC conductance (G_{DC}) was determined from the resulting current step. A 320 Hz, 30 mV peak-to-peak sinusoid was superimposed onto the repeating voltage steps and the resulting sinusoidal current decomposed with a lock-in amplifier (Neher and Marty, 1982) into two components. One (90° out-of-phase with the voltage sinusoid) monitored changes in capacitance (C), more precisely the imaginary portion of the electrical admittance between the inside and the outside of the fibroblast. The other (in-phase) monitored changes in AC conductance (G_{AC}), or the real portion of the admittance. At the beginning of each experiment, a 2 pF deflection was applied to the cell for calibration, and electrical delays in our recording equipment and in the pipette–cell junction were cancelled by adjusting the phase on the lock-in amplifier such that the 2 pF capacitance change produced no change on the G_{AC} trace. At the end, another 2 pF deflection was applied; the accompanying deflection in the G_{AC} trace was always 17-fold smaller than the C deflection, indicating that the phase setting had remained adequate. The voltage and current pulses and the C and G_{AC} signals were stored on a four-channel FM tape recorder (4DS; Racal Health & Safety, Inc., Frederick, MD) for later analysis on a digital computer.

Video Microscopy

Cells were viewed on an inverted microscope (Diaphot; Nikon, Melville, NY) equipped for epifluorescence (rhodamine filter cube G2A for TR-DPPE; 650 nm filter cube) (Omega Optical Inc., Brattleboro, VT) with 633-nm band pass excitation filter and 665-nm low pass barrier filter for di-I). Fluorescence was excited by a 50 W quartz-halogen lamp with regulated DC power supply. Images were formed by a 100×/1.3 NA oil immersion objective (Neofluar; Carl Zeiss, Oberkochen, Germany), passed through an image intensifier (KS 1381; Video Scope Intl., Washington, DC) and were recorded by a CCD camera (XC-77; Sony, Montvale, NJ). Both the image intensifier and the camera were set at maximum gain when viewing fluorescence; for brightfield images, the gain of the image intensifier was occasionally reduced 10-fold. Video images were captured by an image processor system (Image-1; Universal Imaging Co., Westchester, PA) that also controlled the illumination of the sample via electronic shutters (VS25; Uniblitz, Vincent Associates, Rochester, NY).

To minimize photodamage, stained cells were illuminated only intermittently and for short periods (340 ms). Because di-I is excited in the far red, RBCs so stained tolerate more intense illumination (Bloom and Webb, 1983) and could be illuminated more frequently. During the 340-nm illumination period, Image-1 acquired eight video frames, averaged them, read the time, entered it into a data table, and stored the averaged image on an optical memory disc recorder (TQ-2028F; Panasonic). Later, Image-1 retrieved the image for analysis and display. All images shown here were photographed from a TV monitor (PVM-1324Q; Sony, Montvale, NJ) displaying single-frame replays from the optical disc.

For analysis, we drew boundaries around the RBC, the fibroblast, and a region containing no cell (background). Image-1 calculated the average brightness of each region (light divided by area) and then entered results into the data table alongside the times at which each image was acquired. Further analysis was done with a spreadsheet (Lotus 1-2-3). To test the linearity of light recording, we illuminated a fluorescent area through a series of calibrated neutral density filters. When we plotted the brightness determined by Image-1 against calibrated light intensity, linear regression gave an r^2 of 0.99, and an intercept not statistically different from zero.

Dependence of Fluorescence on Voltage and pH

Since the activation of the HA requires acidification, and since the membrane potential of the RBC changes when the fusion pore opens (Spruce et al., 1991), we tested the effect of pH and membrane potential on our lipid probes. Stained RBCs were bound to untrypsinized fibroblasts that could not fuse to RBCs, and hence did not take up the probe after acidification. Acidification caused no change in fluorescence (<0.25%/min; n = 2 for each TR-DPPE and di-I). To test for voltage dependence of fluorescence, stained RBCs attached to untrypsinized fibroblasts were voltage clamped with pipettes that were filled with internal solution, had 15–20 MΩ resistances and made >30 MΩ connections with the cytosol. TR-DPPE fluorescence did not change with voltage between −80 mV and +80 mV (n = 2) at pH, 4.8. Di-I fluorescence increased by up to 3% within 1 s after switching from 0 to +40 mV but did not change thereafter.

Dequenching of octadecylrhodamine (R18) fluorescence has been extensively used to monitor fusion (Hoekstra et al., 1984; Sarkar et al., 1989). When incubated for 15 min at 25°C in PBS with 1–2 μl/ml of ethanolic R18 stock (1 mg/ml), RBCs fluoresced brightly. However, acidification caused a slow decline of fluorescence (2.2 and 3.5%/min, n = 2) in the absence of fusion. Changing the RBC membrane voltage from 0 to +80 mV increased the fluorescence 3–4%/min over several minutes, and a potential change to −80 mV decreased the fluorescence at a similar rate. Moreover, we occasionally observed that stained RBCs donated fluorescence to fibroblasts although electrical recordings gave no sign of fusion; this was never observed with the other two dyes. Because of these complications, use of R18 was abandoned.

Results

Detection of Single Fusion Events by Voltage Clamp and Fluorescence Imaging

Figs. 1 (*a* and *c*) and Fig. 2 demonstrate fusion of a fibroblast to an erythrocyte (RBC) stained with the fluorescent lipid di-I. In Fig. 1 *a* (top trace), fusion was detected by measuring C, the imaginary portion of the admittance of the fibroblast, which is proportional to the plasma membrane capacitance. Mild trypsinization had made the HA on the fibroblast's surface fusion-competent, and a single RBC had

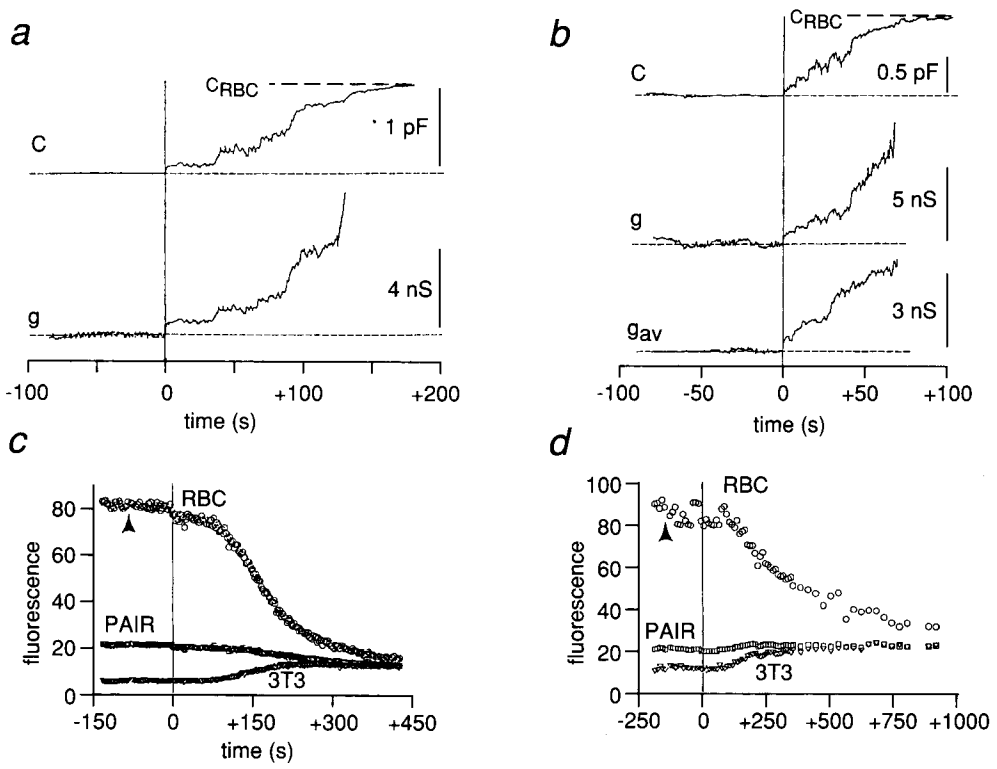

Figure 1. HA-mediated fusion of fibroblasts to single erythrocytes (*RBCs*), stained with di-I (*a* and *c*) or TR-DPPE (*b* and *d*). (*a*) Upper trace, plasma membrane capacitance (*C*) measured as the imaginary part of the electrical admittance between cytosol and extracellular fluid. Extracellular fluid was acidified at the start of the trace; the small but abrupt increase in capacitance ($t = 0$) marks the onset of fusion. Lower trace, conductance, g, of the HA-mediated electrical connection between the two cells, calculated from ΔC, the capacitance change, by (e.g., Spruce et al., 1991)

$$g = \frac{2\pi f(\Delta C\, C_{RBC})^{1/2}}{(1 - \Delta C/C_{RBC})^{1/2}} \qquad (1)$$

where f is the frequency of the sinusoid (320 Hz). C_{RBC} (*dashed line*) is the capacitance of the RBC estimated from the final value of ΔC (Spruce et al., 1989) and was 1.11 pF in this experiment. The fibroblast's initial capacitance was 8.3 pF; the conductance of the pipette–fibroblast junction was 0.13 μS at the beginning and 0.11 μS at the end of the experiment. (*b*) Upper two traces (*c* and *g*) obtained as in *a* but with the RBC were stained with TR-DPPE. Initial capacitance 18 pF, conductance of the pipette–fibroblast junction 0.30 μS from beginning to end. Lowermost trace, average conductance (g_{AV}) of the RBC-fibroblast junction in 6 similar experiments with TR-DPPE stained RBCs. (*c* and *d*) Fluorescence (arbitrary units) of the two RBCs and fibroblasts (3T3) analyzed in *a* and *b*, respectively; the fluorescence averaged over each cell pair is also shown. Time relative to the onsets of fusion determined in *a* and *b*. Arrowheads mark the time of acidification. For sample images from the experiment in *c* see Fig. 2. Light was collected from, and divided by, the areas marked in Fig. 2; background fluorescence subtracted throughout. In *c*, the fluorescence of the cell pair began to decline slightly 150 s after fusion. This was due to labeled lipid moving into areas of fibroblast membrane that were sucked into the pipette tip during seal formation and breakthrough. The pipette tip was slightly out of focus and its fluorescence collected at lesser efficiency.

bound to it. 81 s after the HA had been activated by acidifying the external medium, C began to increase in successive episodes, twice abruptly and then more gradually. The time origin marks the beginning of fusion as judged from the C trace. Previous work (Spruce et al., 1989) has shown that the capacitance increase is due to the HA-mediated fusion of RBC and fibroblast, hence the 1.11 pF increase in Fig. 1 *a* (C_{RBC}) represents the addition of 111 μm² of RBC membrane.

For fusion to be detected in this assay, the sinusoidal voltage used to measure C must propagate through the fusion pore from the fibroblast into the RBC. While the pore and its electrical conductance are small, the sinusoid cannot invade the RBC efficiently; only when both become large is the membrane capacitance of the RBC fully revealed. As the conductance of the electrical connection between the two cells increases and becomes immeasurably large, C grows to its final value, C_{RBC}. In Fig. 1 *a* (lower trace), this conductance (*g*) was calculated from the C trace as described (Spruce et al., 1989, 1991). As the first fusion pore opened, g rose abruptly to 0.64 nanosiemens (nS). The later, similarly abrupt increase to 1.33 nS probably reflects the opening of a second pore (see also Spruce et al., 1991). Later the conductance increased more gradually as if one or both pores dilated.

Cell fusion also allows the exchange of lipids between the bilayers surrounding the fusing cells, and this can be observed as the movement of a fluorescent lipid from one cell into another (Sarkar et al., 1989). Fig. 2 *a*(*1*) shows the cell pair from which the recordings of Fig. 1 *a* were made. The RBC had its bilayer stained with di-I, a fluorescent lipid (Fig. 2 *b* (*1* and *2*), and fusion allowed di-I to move into the fibroblast. However, movement of di-I was delayed relative to the electrical signs of fusion; the times at the bottom of Fig. 2 are relative to the time origin in Fig. 1 *a*. As late as 92 s after the first fusion pore had opened (Fig. 2 *b*,*2*), fluorescence remained confined to the RBC in this experiment. Only after 198 s was di-I clearly present in the fibroblast (Fig. 2 *b*,*3*) and by +443 s, di-I had distributed evenly over the two cell membranes (Fig. 2 *b*,*4*). The outline of the RBC on the fibroblast became somewhat more rounded but remained clearly visible (Fig. 2 *a*,*4*) even though the fusion pore had become so large that g could no longer be measured.

To quantify the spread of fluorescence, boundaries were drawn around the RBC and the fibroblast (Fig. 2 *c*,*1–4*). Fig. 1 *c* tracks the brightness of the two areas thus enclosed, as well as the average brightness of both cells combined. About 90 s after acid was added (*arrowhead*), the first fusion pore opened ($t = 0$), and the fluorescence of the RBC diminished slightly but abruptly. The small but abrupt loss of fluores-

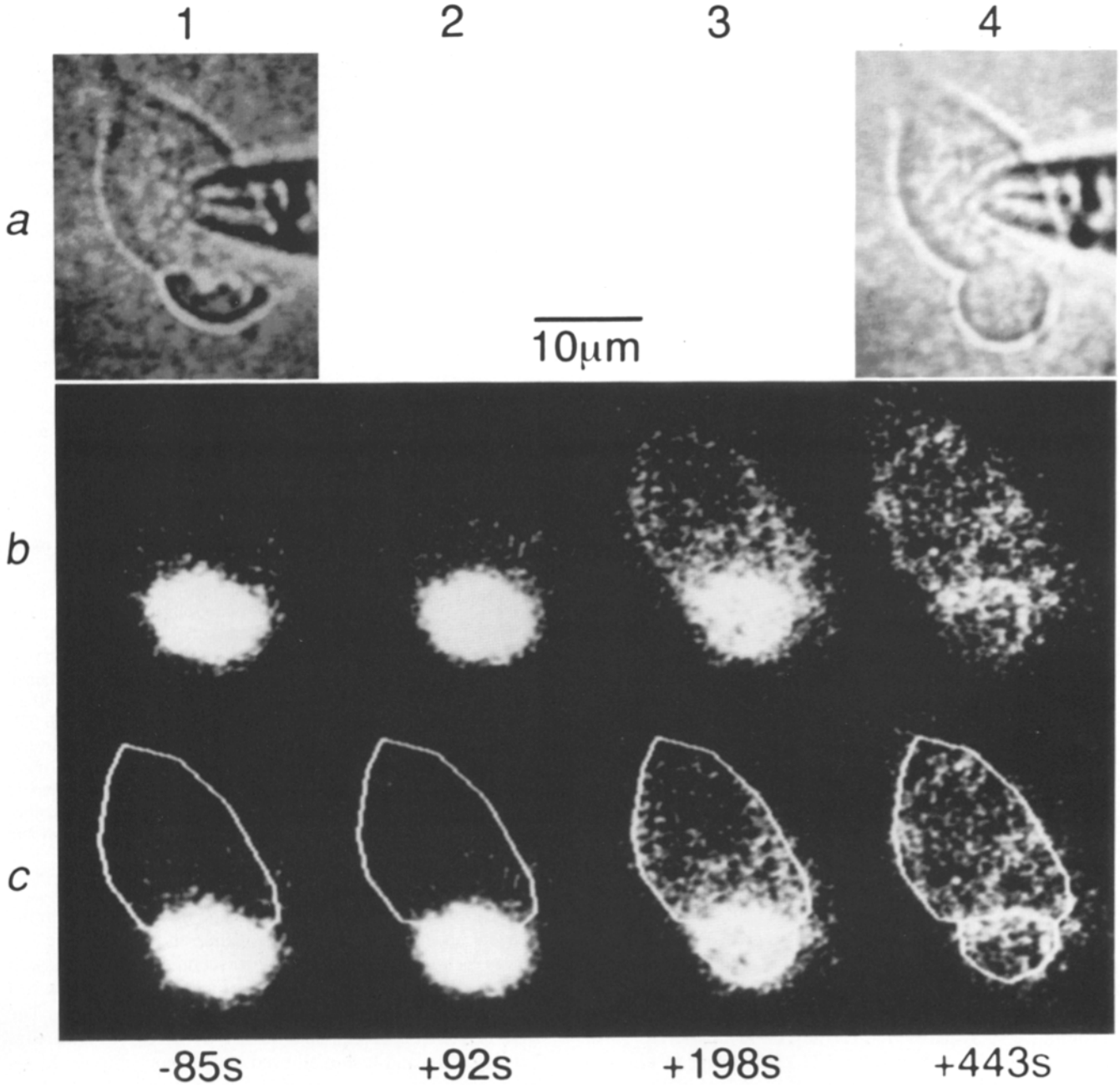

Figure 2. Lipid flux in a fusing fibroblast–RBC cell pair. (*a*) Brightfield images of the cell pair investigated in Fig. 1 (*a* and *c*) taken near the beginning and end of the experiment. The patch pipette used for electrical recording is seen at the right; the RBC, stained with the fluorescent lipid di-I, lies beneath the fibroblast. (*b*) Fluorescence images of *a* at various times (*bottom*) relative to the beginning of fusion measured electrically in Fig. 1 *a*. The first image was captured just after HA was activated by acidification, the others at various times after fusion. (*c*) Boundaries were drawn around fibroblast and RBC, and the brightness of the two areas (light divided by area) was measured. Background measured in a third region containing no fluorescent material (not shown) was subtracted. The boundaries were drawn once, but those of RBC and fibroblast were occasionally moved as a unit to compensate for movements of the cell pair, caused by thermal drift of the heated microscope stage. While the investigator moved the boundaries in a video frame, he did not know at what time relative to fusion the frame was recorded.

cence does not represent loss of lipid into the fibroblast, because light collected from that cell decreased also, and by the same fractional amount. Instead, the effect almost certainly arose because the RBC, initially inside positive under our experimental conditions (Spruce et al., 1991), lost its membrane potential as it became electrically connected to the fibroblast (see Materials and Methods).

For the next 90 s, fluorescence of the RBC changed little. Later, however, the fluorescence of the RBC diminished while that in the fibroblast grew. Ultimately the lipid probe distributed evenly over both cell membranes and both became equally bright. The average final time constant with which di-I equilibrated was 67.3 ± 9.7 s in the four experiments where the increase in C went to completion, as in Fig.

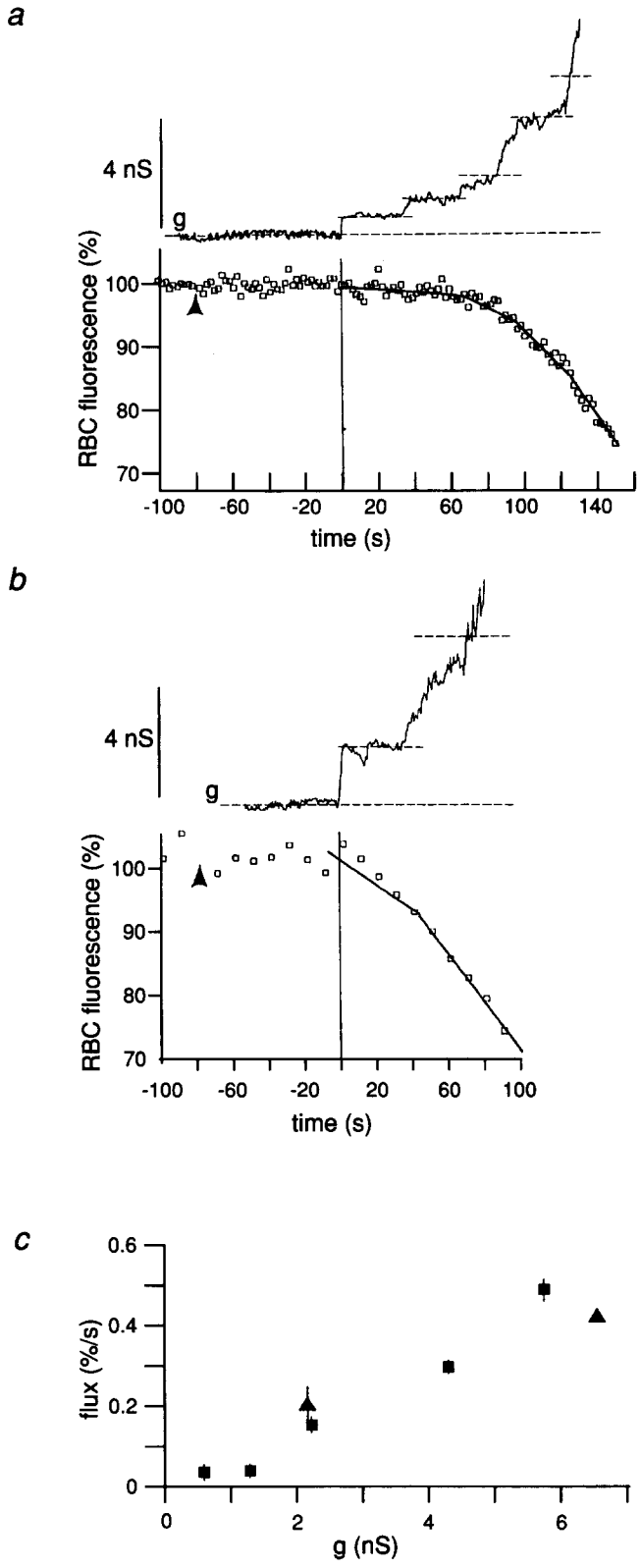

Figure 3. Comparison of membrane flux and junctional conductance. (*a*) From the cell pair of Figs. 1 *a* and *c* and 2. Conductance (*g*) and RBC fluorescence traces were each divided into five segments (0 to 36 s, 36 to 66 s, 66 to 95 s, 95 to 124 s, and 124 to 147 s). For each segment, we calculated the average conductance (*dashed lines*) as well as the rate constant of lipid flux by fitting a straight line to the fluorescence trace and dividing its slope by its initial value. To join the lines, points to the left and the right of each segment (3 points each in *a*, one point each in *b*) were included in the fit. Several small effects unrelated to the movement of lipid could potentially affect RBC fluorescence; these include photobleaching, membrane potential changes in the RBC, and changes in the intensity of fluorescence excitation. To correct for them, the trace in *a* has been divided by the fluorescence of the cell pair; it was then normalized to the average of all measurements taken at $t < 0$. (*b*) As in *a* but from another fusion where the pore conductance rapidly increased to large values and the RBC started to lose fluorescence immediately. (*c*) Rate constant of lipid flux as a function of average junctional conductance for the five segments in *a* (*squares*) and the two segments in *b* (*triangles*).

1. The fluorescence of the cell pair changed little if at all; unlike another dye used in previous work (R18, e.g., Sarkar et al., 1989), di-I moved into the fibroblast without increasing its fluorescence by dequenching. Similar results were obtained in 13 other experiments.

Fig. 1 (*b* and *d*) illustrates a similar experiment where the RBC was stained with TR-DPPE, the fluorescent derivative of a naturally occurring lipid. Again, a slow increase in capacitance by about 1 pF (Fig. 1 *b*, top trace) demonstrates the opening and subsequent dilation of a fusion pore; its conductance (g) is shown in the middle trace. The bottom trace shows the average of six such experiments (g_{av}); a relatively abrupt rise to 0.45 nS is followed by a more gradual increase that continues until g is too large to measure with our method. Fig. 1 *d* analyzes fluorescence measurements on this cell pair made as in Fig. 2. Again, little or no dye was lost for minutes after the fusion pore had opened. Only later did the fluorescent lipid distribute evenly across the two cell membranes. The average time constant (259 ± 54 s, $n = 4$) was about four times larger than with di-I ($P < 0.05$, one-tailed *t* test).

Lipid Flux Requires a Threshold Pore Conductance

Fig. 3 *a* continues the analysis of the fusion in Fig. 1 *a* and Fig. 2, plotting junctional conductance (g) and RBC fluorescence against time. The rate at which di-I is lost into the fibroblast was measured by fitting regression lines to segments of the fluorescence curve and measuring their slope (see legend of Fig. 3 for details). Fig. 3 *c* plots the rate constant of lipid flux against junctional conductance (*squares*). Lipid flux was not detectable while the conductance remained below 1.4 nS, but as the conductance increased beyond this value, flux increased in parallel. Fig. 3 *b* shows another, similar experiment where the junctional conductance rapidly increased to large values, and lipid flux started immediately. When this experiment was analyzed as in Fig. 3 *a*, similar flux rates were obtained for similar conductances (Fig. 3 *c*, triangles). Evidently, lipid flux depends more on the junctional conductance than on the time since a pore first opened.

Fig. 4 summarizes 13 similar experiments with di-I, including those in Fig. 3. If the conductance arose from a single pore, it would be proportional to the cross-sectional area of the pore, and the square root of the pore conductance proportional to the pore diameter (or circumference). Therefore, the junctional conductance on the abscissa is plotted on a square root scale. Since lipid flux is expected to be proportional to the pore circumference (see Discussion), the theo-

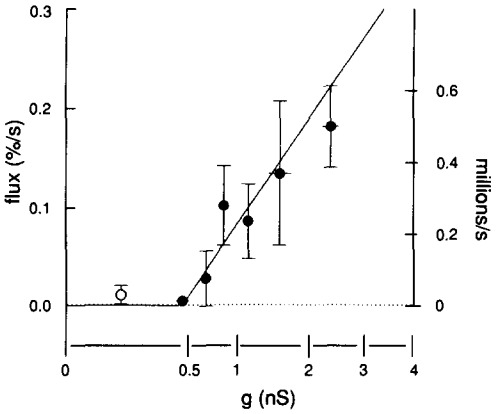

Figure 4. Membrane flux requires a threshold pore conductance. Summary of 13 experiments as in Fig. 3. Conductance plotted on a square root scale. Vertical error bars indicate SE where larger than the symbol, horizontal error bars 1 SD. Each filled circle represents four to six segments, the open circle a single measurement. The line is a fit to the individual measurements, all weighted equally. With 217×10^6 phospholipid molecules per RBC (van Deenen and deGier, 1974), 0.1%/s would correspond to 0.217×10^6 molecules/s if all phospholipids in both leaflets of the RBC bilayers diffused at the same rate as di-I. This defines the right-hand ordinate.

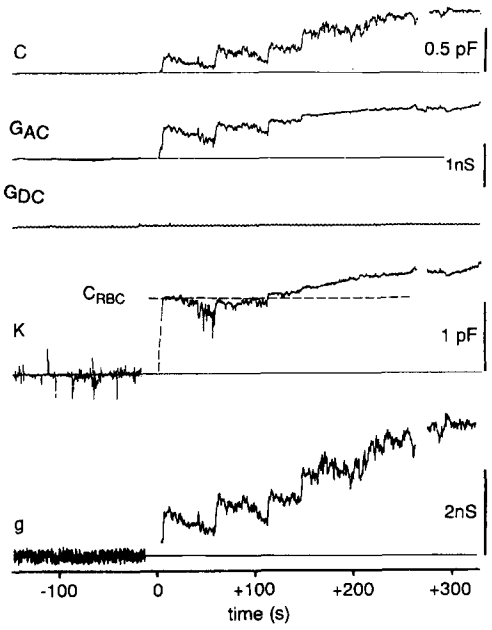

Figure 5. Fusion pores occasionally fail to dilate. C, imaginary (capacitance) and G_{AC}, real portion (AC conductance) of the electrical admittance of a fibroblast; G_{DC}, DC conductance of the fibroblast plasma membrane, measured with 0.5 s square pulses (see Materials and Methods). The trace labeled K represents the variable

$$K = [\Delta C^2 + (\Delta G_{AC}/2\pi f)^2]/\Delta C \quad (2)$$

where ΔC and ΔG_{AC} are the fusion-related changes in C and G_{AC}. Theoretically, K is a step with amplitude C_{RBC} (Lindau, 1991); deviations represent experimental uncertainty. The dashed line (1.10 pF) was fit to the early portion of the experiment which we consider most reliable. Bottom trace, junctional conductance (g) calculated by eq. (1) using the value of C_{RBC} estimated above; g does not depend critically on the estimate of C_{RBC} while $\Delta C \ll C_{RBC}$. Capacitance calibrations were performed immediately before the opening of the first fusion pore and 280 s later, hence, the gaps in the traces. Initial capacitance of the fibroblast 15.0 pF, conductance of the pipette–cell junction 0.19 μS at the beginning and 0.18 μS at the end of the experiment. RBC stained with TR-DPPE.

retically expected relationship between flux and the square root of the conductance is a straight line. The regression line in Fig. 4 intersects the abscissa at a conductance of 0.47 nS, the average threshold conductance for lipid flux; the correlation is statistically significant ($P < 0.005$).

At conductances above 0.5 nS, error bars are large. Much of the variability is due to fusions where large conductances were not associated with measurable lipid flux, and where the recordings suggest that the conductance grew due to the successive opening of several fusion pores (e.g., Figs. 1 *a* and 4; see also Fig. 2 of Spruce et al., 1991). The largest lipid-impermeable junction of this kind had a conductance of 2 nS. If these fusions are ignored, the regression line is steeper, but the conclusion that there is no measurable flux through a junction below 0.5 nS is still valid.

An Upper Limit for Lipid Flux through a Small Fusion Pore

Occasionally, the junctional conductance remained small for minutes, as if fusion pores failed to dilate. An example is shown in Fig. 5, obtained with a RBC stained with TR-DPPE. C, G_{AC}, and G_{DC} are plotted against time. G_{DC}, the conductance measured with voltage steps, remains negligible throughout, hence G_{AC}, measured with a sinusoid, must have been entirely due to resistive elements with a membrane in series, i.e., due to fusion pores. Presumably because the junctional conductance remained small in this fusion, C never increased by the amount expected from a RBC, and C_{RBC} could not be obtained as the final asymptote of the C trace as in Fig. 1. Instead C_{RBC} was estimated by considering both the C and G_{AC} traces (dashed line in Fig. 5, see legend). The junctional conductance (g) is seen to increase in jumps suggestive of the opening of several fusion pores in succession.

Fig. 6 shows fluorescence micrographs of the cell pair of Fig. 5, acquired at the indicated times before and after the opening of the first fusion pore. For more than 6 min after fusion, TR-DPPE transfer remained undetectable. Some flux may have occurred ~11 min after fusion, but the experiment had to be abandoned before the TR-DPPE could equilibrate. Images were analyzed as in Figs. 1 *c* and 2 *c*, and the normalized fluorescence of the RBC plotted against time. A regression line fitted to the first 360 s after fusion (not shown) indicated a flux rate constant of -0.0028 ± 0.0029%/s, not statistically different from zero. Any rate constant larger than 0.0056%/s (i.e., two standard errors) would have been detected, hence the RBC in Figs. 5 and 6 lost TR-DPPE at a rate of <0.0056%/s.

Experiments with di-I led to a similar conclusion. Fig. 7 was compiled from nine fluorescence traces, including that in Fig. 3 *a*. Segments where the junctional conductance remained <0.8 nS were selected and averaged. A regression line fitted to the points after fusion had a slope of $+0.0017 \pm 0.0024$%/s. Any slope more negative than -0.0048%/s (i.e., two SE) would have been detected, hence di-I is lost

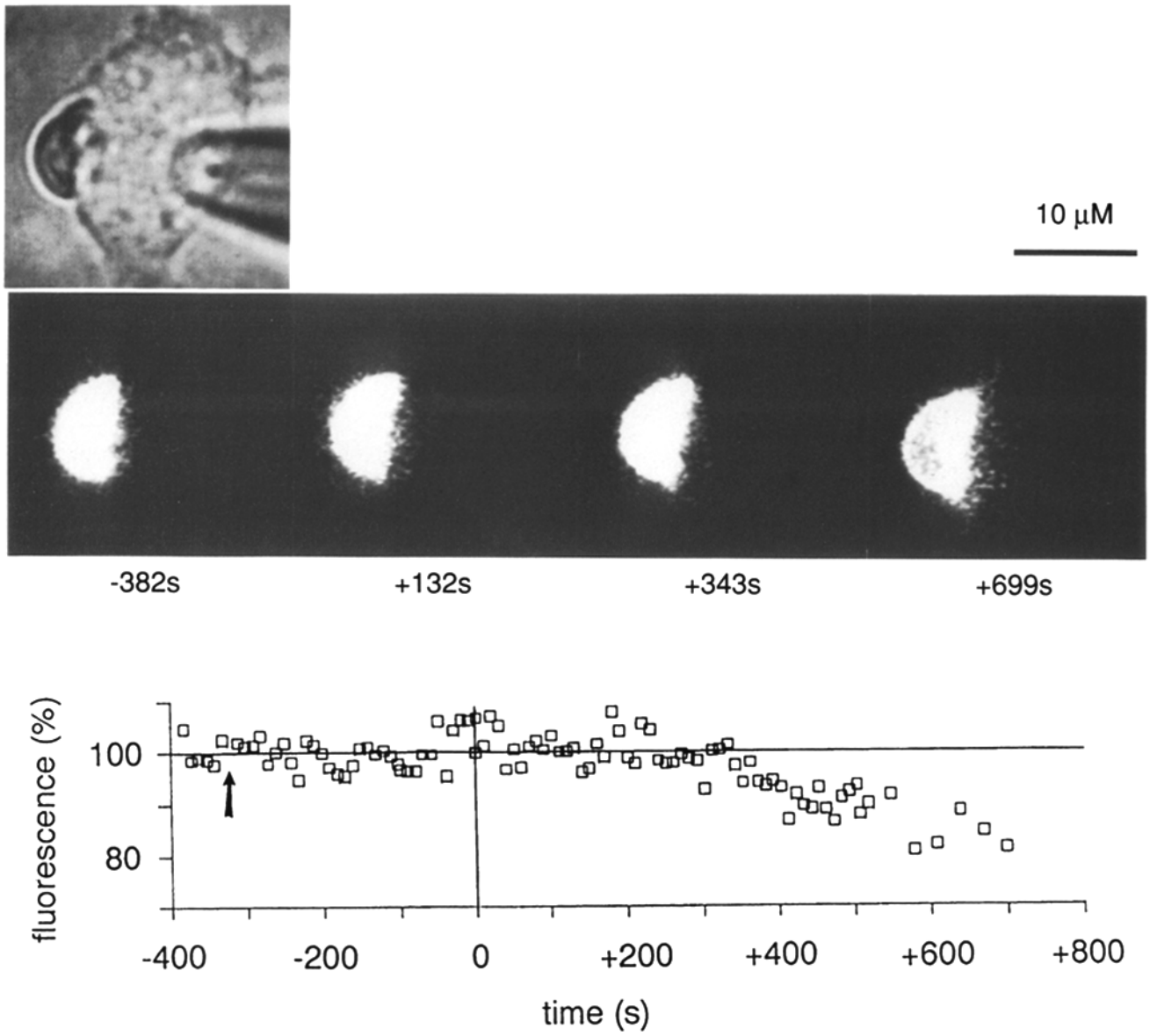

Figure 6. Brightfield (*top*) and fluorescence images (*middle*) of the RBC in Fig. 5; times are given relative to the first opening of a fusion pore in Fig. 5. (*Bottom*) Fluorescence of the RBC, obtained as described for Figs. 1 *A*, 2 and 3 *A* (see legends). Acid applied at the arrow.

through small fusion pores at a rate of <0.0048%/s. If all of a RBC's phospholipids diffused at the same speed as di-I, 0.0048%/s would correspond to a flux of ~10,000 molecules/s.

Discussion

When mediating cell fusion, HA forms an aqueous connection (fusion pore) between the fusing cells (Sarkar et al., 1989; Spruce et al., 1989, 1991), and allows lipid flux from the plasma membrane of one cell to that of the other (Sarkar et al., 1989). We have correlated lipid flux with the electrical conductance (and with the diameter) of the fusion pore. We have used two lipid probes, di-I and TR-DPPE, the fluorescent derivative of a naturally occurring lipid. Our data on di-I are more extensive, but both dyes gave qualitatively similar results. Large pores readily pass lipid, and drain RBCs of the fluorescent lipids di-I and TR-DPPE with time constants of 63 and 260 s, respectively. The difference between the two values must be related to the larger polar headgroup of TR-DPPE, as the two molecules are otherwise nearly identical. This suggests that the diffusion of TR-DPPE is hindered by structures outside the lipid bilayer. With di-I, even moderately sized pores with 2–3 nS conductance can pass 400,000 molecules/s and must, therefore, be at least partly lipidic.

Membrane flux has been observed also along exocytic fusion pores by Monck et al. (1990) during transient fusion events in mast cells. They saw a net flux of 600,000 lipid molecules/s from the plasma membrane into the secretory vesicle. The pore conductance was not measured, but is likely to have been several nanosiemens since the transient fusion events analyzed by them caused capacitance changes approaching the capacitance of single vesicles. In their work, too, fusion pores must have been partly or largely lipidic.

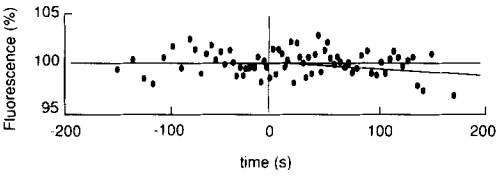

Figure 7. Lipid flux through small fusion pores. Analyses on nine fusions with di-I stained RBCs were carried out as in Figs. 1 *A*, 2, and 3 *A*. Segments with junctional conductances of <0.8 nS were averaged. In two fusions, one of them illustrated in Fig. 1 *a*, junctional conductances increased in steps suggestive of the successive opening of two or more fusion pores; in these cases, measurements at higher junctional conductances were also included. A regression line fitted to points after fusion had a slope of −0.0007 ± 0.0024%/s. The sloping line has a slope of two standard errors, or −0.0048%/s. It represents our limit of detection; any steeper downward slope would have been detected with 95% probability.

However, HA-mediated fusion pores opened well before the mixing of membrane lipids could be detected. Fusion began with pores of 0.3–0.8 nS conductance, and through such early pores no lipid flux was seen. Evidently small pores pass little or no lipid. Restricted motion of lipids through fusion pores could explain also the unexpectedly slow escape of dye R-18 from the viral envelope (Giorgiou et al., 1989; Lowy et al., 1990).

Models of the Early Fusion Pore

Hypotheses as to the structure and formation of the early fusion pore fall in two classes. In the first, the only function of HA is to bring two bilayers so close together that they fuse on their own. Fusion starts with a lipidic intermediate (perhaps an "inverted micellar intermediate", Fig. 8 *A, 1,a,b*; Rand & Parsegian, 1986), that later opens into an electrolyte-filled tube (Fig. 8 *A, 2,a* and *b*). Soon the tube expands (Fig. 8 *A, 3,a* and *b*) and ultimately becomes as large as the compartments it connects. Here, the fusion pore is lipidic from the start. In any model of this kind, lipids in the outer leaflet should begin to mix before the fusion pore opens. When it opens, the rate of mixing may increase only insignificantly insofar as the opening of the pore demands a small increase in circumference of the contact zone. As the pore expands its inner diameter (Figs. 8 *A, 3,a* and *b*), circumference and flux increase in proportion (Fig. 8 *B*).

In the second class of hypotheses, the aqueous connection between the fusing compartments is initially formed by a structure that is partly or entirely proteinaceous. For illustration we consider a particularly simple version that was proposed to explain the rapid exocytosis of synaptic vesicles (Almers, 1990; Almers and Tse, 1990). In applying it to HA-mediated fusion, we assume that HA molecules (or parts thereof) insinuate themselves into the bilayer of the target cell, and aggregate to form a macromolecular bridge spanning the bilayers of both, RBC and fibroblast (cross-section shown in Fig. 8, *C,1*). Once in place, the HA molecules form an aqueous channel in their midst (Fig. 8 *C,2*), much as the subunits of the gap junction channel form a proteinaceous cell–cell junction. Only later does the pore dilate by incorporating lipids into its circumference (Fig. 8 *C,3*). In this model, lipid mixing must wait until the fusion pore has not only opened but also dilated, and until a continuous lipidic path between the fusing membranes has been formed. Again, lipid flux increases linearly with inner pore diameter, but this time the line intersects the abscissa, the intercept being the diameter of the early fusion pore (Fig. 8 *B*).

Even Small Lipidic Pores Are Expected to Allow Large Lipid Fluxes

Fig. 4 clearly agrees better with the second hypothesis. Nonetheless, we now ask whether our method would have detected flux through single lipid pores. To estimate this flux, we view lipid flow as facing two barriers, one arising in the pore itself, the other representing the difficulty of access and egress from the two entrances of the pore. Note that labeled lipid was applied only to the outside of the RBCs, so that both TR-DPPE (van Meer and Simons, 1986) and di-I (Wolf, 1985) are expected to have stained only the outer bilayer leaflet.

To calculate a lower limit for lipid flux, we assume that the inner diameter of the lipidic pore is infinitesimally small (Fig. 8 *A,1,c* and *d*). This physically unlikely structure would have an outer diameter at least two bilayers wide (8.2 nm), and its circumference (26 nm) would accommodate 32 phospholipid headgroups (0.8-nm diam). If the pore connecting the lumina of the fusing compartments were as long as the entire HA trimer (20.5 nm; Ruigrok et al., 1986), then the distance between the outer bilayers would be 12.3 nm (20.5 nm minus twice the thickness of a bilayer). With a diffusion coefficient of 1 $\mu m^2/s$ in RBC plasma membrane (Bloom and Webb, 1983), a di-I molecule diffuses 12.3 nm in 76 μs. Hence, at least 423,000 di-I molecules/s would pass through a fusion pore surrounded by 32 molecules, provided they are replenished instantly at one end of the pore and vanish instantly at the other. There are 117×10^6 phospholipids in the outer membrane leaflet. If they were replaced with 117×10^6 di-I molecules, a RBC would lose di-I with a rate constant of 0.36%/s, and a time constant of 277 s. For a pore shorter than the entire length of a HA-molecule the diffusion time would be less and the rate constant larger.

The rate at which lipid molecules arrive and leave at the entrances of a pore was calculated by Rubin and Chen (1990) who analyzed the time course with which a RBC loses a lipid probe through an infinitesimally short pore. For small pores, this happens approximately exponentially. We have used equation (B27) of Rubin and Chen (1990), and assumed that a 7-μm-diam RBC equilibrates with a 20-μm-diam fibroblast through a collapsed lipid pore (4-nm center-to-center distance of the bilayer walls; see Fig. 8 *A,1,c* and *d*). In this calculation the lipid probe equilibrates with a rate constant of 0.28%/s and a time constant of 357 s. Since the two barriers are in series, the time constants add, and we calculate an overall rate constant of 1/634 s or 0.16%/s. Instead, no flux was observed. Loss of di-I from a RBC at a rate of 0.0048%/s would have been detected, therefore the flux actually occurring (if any) must be at least 30 times less than expected for the smallest conceivable lipidic pore.

Small Fusion Pores Are Surrounded by Protein

In Fig. 4, the threshold conductance for lipid flux is ~0.5 nS. On the time scale of experiments as in Fig. 1 (see also Spruce et al., 1989, 1991), the first fusion pore appears to open to a conductance of 0.3–0.8 nS, and often remains at that level for tens of seconds or minutes without passing

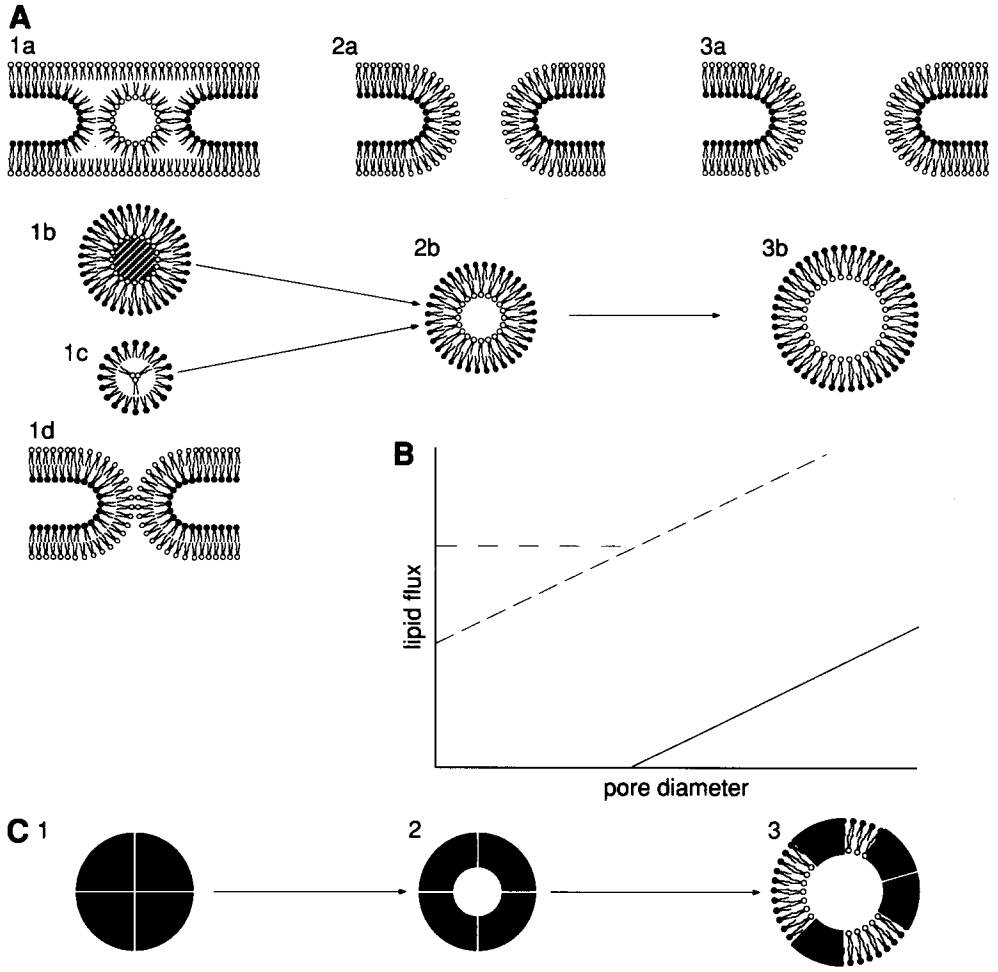

Figure 8. Two models of a fusion pore. (*A*) Fusion without proteins. The fusion junction is sectioned perpendicular to the bilayers (*1a–3a*) or in a plane parallel to and midway between the bilayers (*1b* and *1c–3b*). The "outer" bilayer leaflet (dark lipid headgroups here and elsewhere) in contact with the extracellular space was stained in our experiments. *1a* and *1b* "inverted micellar intermediate" (e.g., Rand, 1981); *2a* and *2b* small pore, and *3a* and *3b* an expanded pore. *1c* and *1d* collapsed pore without internal opening, an alternative to *1a* and *1b*. This structure seems physically unlikely and we use this smallest conceivable lipidic pore only to calculate a lower limit of lipid flux (see text). (*B*) Relationships expected between lipid flux and inner pore diameter. Dashed lines are for model A; widely separated dashes represent the transition from *A 1a* and *1b* to *A 2a* and *2b* where an aqueous connection forms without an increase in outer diameter. The continuous line represents the model described in *C*. (*C*) Fusion mediated by a lipid-impermeable (e.g., proteinaceous) fusion pore complex, cross-sectioned with the plane of section as in *A 1b* and *1c–3b*. *1* before, and *2* after the opening of a small fusion pore. *2* contains no mobile lipid and hence does not allow lipid flux. *3*, pore has expanded by inclusion of mobile lipid in the circumference; the lipid patches, if continuous from one end of the pore to the other, allow lipid flux.

lipid. In recordings on a millisecond time scale (Spruce et al., 1991), still smaller HA-mediated fusion pores are regularly observed. They open abruptly to an average level of 150 pS and increase their conductance to ~0.5 nS in tens or hundreds of milliseconds. It is likely that these very early structures are similarly impermeable to lipid.

We have shown that early fusion pores prevent or restrict the mixing of lipids between the outer leaflets of fusing bilayers. In early pores, di-I moves at <1/30th the speed measured within the lipid bilayer of a RBC. Our results are consistent with early fusion pores being either entirely proteinaceous (Almers and Tse, 1990; Guy et al., 1992) or proteinaceous channels whose lumen is covered with a lipid monolayer (White, 1990; Pollard et al., 1991). We cannot exclude that the outer leaflet of the pore wall is lipidic, but then the lipids must be immobile, and this is difficult to imagine other than through interaction with a ring of protein inside it or around it. Put most simply, our results suggest that pores of up to 0.5 nS conductance are surrounded by a ring of protein. Pores dilate by breaking this ring and by incorporating lipid into their circumference.

Which part of the HA ectodomain forms the pore? When HA is made fusion competent by hydrolytic cleavage, one of the hydrolysis products ends in a hydrophobic segment 24 amino acids long. This so-called "fusion peptide" is essential for fusion (Stegmann et al., 1989; White, 1990) and, by photolabeling, is known to be the only part of the ectodomain that contacts a hydrophobic environment for extended periods during fusion (Harter et al., 1989). Labeling suggests that the fusion peptide is a helix, and that a stripe along the helix remains in a hydrophilic environment. These studies fit with models where several HA trimers (Ellens et al., 1990) contribute enough helical fusion peptides to enclose a pore much as staves enclose a barrel. The hydrophilic stripe may face the extracellular space and the hydrophobic side a lipid monolayer lining the pore (White, 1990). Alternatively, the hydrophilic side may face the aqueous lumen of the pore, and the hydrophobic side a lipid monolayer surrounding it. Whether these views are correct remains to be seen. A large number of fusion peptides may be required to line a pore large enough to have a 0.5 nS conductance. Also, a helical fusion peptide would be long enough to span only a single bilayer. Other parts of HA (e.g., the transmembrane segment) may participate in forming the pore.

We thank Drs. Amy Tse and Manfred Lindau for their critical reading of the manuscript.

This work was supported by National Institutes of Health grant GM-39520.

Received for publication 6 November 1992 and in revised form 18 January 1993.

References

Almers, W. 1990. Exocytosis. *Annu. Rev. Physiol.* 52:607–624.

Almers, W., and F. W. Tse. 1990. Transmitter release from synapses: does a pre-assembled fusion pore initiate exocytosis? *Neuron.* 4:813–818.

Almers, W., L. J. Breckenridge, A. Iwata, A. K. Lee, A. E. Spruce, and F. W. Tse. 1991. Millisecond studies of single membrane fusion events. *Ann. N.Y. Acad. Sci.* 635:318–327.

Bloom, J. A., and W. W. Webb. 1983. Lipid diffusibility in the intact erythrocyte membrane. *Biophys. J.* 42:295–305.

Breckenridge, L. J., and W. Almers. 1987. Currents through the fusion pore that forms during exocytosis of a secretory vesicle. *Nature (Lond.).* 328: 814–817.

Doxsey, S. J., J. Sambrook, A. Helenius, and J. White. 1985. An efficient method for introducing macromolecules into living cells. *J. Cell Biol.* 101:19–27.

Ellens, H., J. Bentz, D. Mason, F. Zhang, and J. White. 1990. Fusion of *Influenza* hemagglutinin-expressing fibroblasts with glycophorin-bearing liposomes: role of hemagglutinin surface density. *Biochemistry.* 29:9697–9707.

Giorgiou, G. N., I. E. G. Morrison, and R. H. Cherry. 1989. Digital fluorescence imaging of fusion of *Influenza* virus with erythrocytes. *FEBS (Fed. Eur. Biochem. Soc.) Lett.* 250:487–492.

Guy, H. R., S. R. Durell, C. Schoch, and R. Blumenthal. 1992. Analyzing the fusion process of *Influenza* hemagglutinin by mutagenesis and molecular modeling. *Biophys. J.* 62(Discussions):95–97.

Hamill, O. P., A. Marty, E. Neher, B. Sakmann, and F. J. Sigworth. 1981. Improved patch-clamp techniques for high resolution current recording from cells and cell-free membrane patches. *Pflugers Arch.* 391:85–100.

Harter, C., P. James, T. Bächi, G. Semenza, and J. Brunner. 1989. Hydrophobic binding of the ectodomain of *Influenza* hemagglutinin to membranes occurs through the fusion peptide. *J. Biochem.* 264:6459–6464.

Hoekstra, D., T. deBoer, K. Klappe, and J. Wilschut. 1984. Fluorescence method for measuring the kinetics of fusion between biological membranes. *Biochemistry.* 23:5675–5681.

Lindau, M. 1991. Time-resolved capacitance measurements: Monitoring exocytosis in single cells. *Quart. Rev. Biophys.* 24:75–101.

Lowy, R. J., D. P. Sarkar, Y. Chen, and R. Blumenthal. 1990. Observation of single *Influenza* virus-cell fusion and measurement by fluorescence video microscopy. *Proc. Natl. Acad. Sci. USA.* 87:1850–1854.

Monck, J. R., G. Alvarez de Toledo, and J. M. Fernandez. 1990. Tension in secretory granule membranes causes extensive membrane transfer through the exocytic fusion pore. *Proc. Natl. Acad. Sci. USA.* 87:7804–7808.

Neher, E., and A. Marty. 1982. Discrete changes of cell membrane capacitance observed under conditions of enhanced secretion in bovine adrenal chromaffin cells. *Proc. Natl. Acad. Sci. USA.* 79:6712–6716.

Pollard, H. B., E. Rojas, R. W. Pastor, E. M. Rojas, H. R. Guy, and A. L. Burns. 1991. Synexin: molecular mechanism of calcium-dependent membrane fusion and voltage-dependent calcium-channel activity. *Ann. N.Y. Acad. Sci.* 635:328–351.

Rand, R. P., and V. A. Parsegian. 1986. Mimicry and mechanism in phospholipid models of membrane fusion. *Ann. Rev. Physiol.* 48:201–212.

Rubin, R. J., and Y. Chen. 1990. Diffusion and redistribution of lipid-like molecules between membranes in virus-cell and cell-cell fusion systems. *Biophys. J.* 58:1157–1167.

Ruigrok, R. W. H., N. G. Wrigley, L. J. Calder, S. Cusack, S. A. Wharton, E. B. Brown, and J. J. Skehel. 1986. Electron microscopy of low pH structure of *Influenza* virus hemagglutinin. *EMBO (Eur. Mol. Biol. Organ.) J.* 5:41–49.

Sarkar, D. P., S. J. Morris, O. Eidelman, J. Zimmerberg, and R. Blumenthal. 1989. Initial stages of *Influenza* hemagglutinin-induced cell fusion monitored simultaneously by two fluorescent events: cytoplasmic continuity and lipid mixing. *J. Cell Biol.* 109:113–122.

Spruce, A. E., A. Iwata, J. M. White, and W. Almers. 1989. Patch clamp studies of single cell-fusion events mediated by a viral fusion protein. *Nature (Lond.).* 342:555–558.

Spruce, A. E., L. J. Breckenridge, A. K. Lee, and W. Almers. 1990. Properties of the fusion pore that forms during exocytosis of a secretory vesicle. *Neuron.* 4:643–654.

Spruce, A. E., A. Iwata, and W. Almers. 1991. The first milliseconds of the pore formed by a fusogenic viral envelope protein during membrane fusion. *Proc. Natl. Acad. Sci. USA.* 88:3623–3627.

Stegmann, T., R. W. Doms, and A. Helenius. 1989. Protein-mediated membrane fusion. *Ann. Rev. Biophys. Biophys. Chem.* 18:187–211.

Stegmann, T., J. M. White, and A. Helenius. 1991. Intermediates in *Influenza* induced membrane fusion. *EMBO (Eur. Mol. Biol. Organ.) J.* 9:4231–4241.

van Deenen, L. L. M., and J. de Gier. 1974. *The Red Blood Cell*, D. M. Surgenor, editor. Academic Press, New York. 147–211.

van Meer, G., and K. Simons. 1986. The function of tight junctions in maintaining differences in lipid composition between the apical and the basolateral cell surface domains of MDCK cells. *EMBO (Eur. Mol. Biol. Organ.) J.* 5:1455–1464.

White, J. M. 1990. Viral and cellular membrane fusion proteins. *Annu. Rev. Physiol.* 52:675–697.

Wiley, D. C., and J. J. Skehel. 1987. The structure and function of the haemagglutinin membrane glycoprotein of *Influenza* virus. *Annu. Rev. Biochem.* 56:365–394.

Wolf, D. E. 1985. Determination of sidedness of carbocyanine dye labeling of membranes. *Biochemistry.* 24:582–586.